Journal of the European Ceramic Society xxx (xxxx) xxx–xxx

Contents lists available at ScienceDirect

Journal of the European Ceramic Society

journal homepage: www.elsevier.com/locate/jeurceramsoc

Original Article

Ti_3SiC_2-Cf composites by spark plasma sintering: Processing, microstructure and thermo-mechanical properties

M.A. Lagos[a,*], C. Pellegrini[b], I. Agote[a], N. Azurmendi[a], J. Barcena[a], M. Parco[a], L. Silvestroni[c], L. Zoli[c], D. Sciti[c]

[a] TECNALIA, Industry and Transport Division, Mikeletegi pasealekua 2, E20009 Parque Científico y Tecnológico de Gipuzkoa, San Sebastián, Spain
[b] Ecole Nationale Supérieure de Céramique Industrielle (ENSCI) 87100 European Ceramics Centre, Limoges, France
[c] CNR-ISTEC, Institute of Science and Technology for Ceramics, Via Granarolo 64, I-48018, Faenza, Italy

ARTICLE INFO

Keywords:
Ceramic matrix composites
Max phases
Interface
Mechanical properties
Sintering
SPS
Spark plasma sintering

ABSTRACT

MAX phases, and particularly Ti_3SiC_2, are interesting for high temperature applications. The addition of carbon fibers can be used to reduce the density and to modify the properties of the matrix. This work presents the densification and characterization of Ti_3SiC_2 based composites with short carbon fibers using a fast and simple fabrication approach: dry mixing and densification by Spark Plasma Sintering. Good densification level was obtained below 1400 °C even with a high amount of fibers. The reaction of the fibers with the matrix is limited thanks to the fast processing time and depends on the amount of fibers in the composite. Bending strength at room temperature, between 437 and 120 MPa, is in the range of conventional CMCs with short fibers and according to the resistance of the matrix and the presence of residual porosity. Thermo-mechanical properties of the composites up to 1500 °C are also presented.

1. Introduction

MAX phases are layered carbides or nitrides with crystal structure of hexagonal symmetry. These materials combine ceramic and metallic characteristics, including high electrical and thermal conductivities, machinability, damage tolerance and good thermal shock resistance [1–4]. Among MAX phases, titanium silicon carbide (Ti_3SiC_2) has roughly half the density of the alloys used in today's jet engines and maintains its creep resistance even at high temperatures [2,5]. In addition, its biocompatibility in combination with the previously mentioned mechanical properties makes Ti_3SiC_2 a promising candidate for bioceramic composites [6]. Moreover, Ti_3SiC_2 can be used as a ceramic binder in cutting tools [7] and it is very interesting for nuclear applications [8].

Different composites have been developed to improve the mechanical properties of Ti_3SiC_2, using different reinforcements like SiC, TiC and SiC whiskers [9–11]. The main improvement achieved is the increase of the hardness and toughness of the material. However, the amount of reinforcement is and the improvements are still limited.

This work presents the fabrication of Ti_3SiC_2 composites reinforced with carbon fibers with the aim of reducing the density and thermal expansion of the composite. The presence of fibers can also affect the thermal shock resistance at high temperature of the composites [12]. The processing route here presented consists of dry mixing of the ceramic powder with chopped fibers followed by densification by Spark Plasma Sintering (SPS). The dry mixing of chopped fibers and ceramic powders offers a low cost and time-saving approach to incorporate reinforcing fibers into a Ceramic Matrix Composite (CMC) avoiding brittle fracture and catastrophic failure of the material [12–16]. The process is easier and faster than continuously reinforced processing like reactive melt infiltration (RMI) [17–19], polymer infiltration and pyrolysis (PIP) [20], chemical vapor infiltration (CVI) [21], etc.

The high reactivity of Ti_3SiC_2 with carbon is well known [22]. However, the short processing time in fast sintering processes like SPS can limit the reaction between the matrix and the fibers, as was reported for UHTCs and carbon fibers [23].

The densification of Ti_3SiC_2 by SPS was studied in different works [24,25] and very high density was obtained, almost full densification. However, the aim of this work is to incorporate a high amount of carbon fibers (up to 40 vol%) and in these conditions, the densification is not trivial.

Other important issue is the homogeneity of the final product and the distribution of the fibers in the composite. In the conventional processing with chopped fibers, the dispersion of the fibers in the

* Corresponding author.
E-mail address: miguel.lagos@tecnalia.com (M.A. Lagos).

https://doi.org/10.1016/j.jeurceramsoc.2019.03.037
Received 15 January 2019; Received in revised form 13 March 2019; Accepted 15 March 2019

Table 1
Characteristics of the commercial carbon fibers.

FIBER REF	average size	thermal conductivity (W/mk)	Electric resistivity (10^{-6} Ωm)	Density (Kg/ m^3)
XN-100-15M	150	900	1.5	2.21
HC-600-15M	150	600	2	2.21

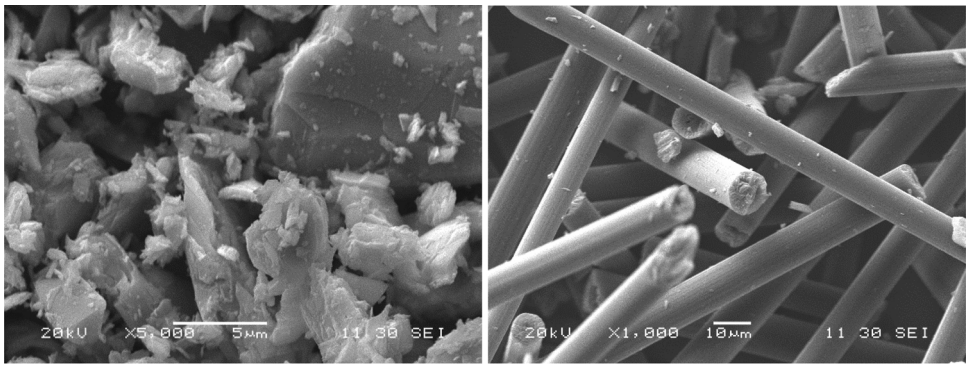

A B

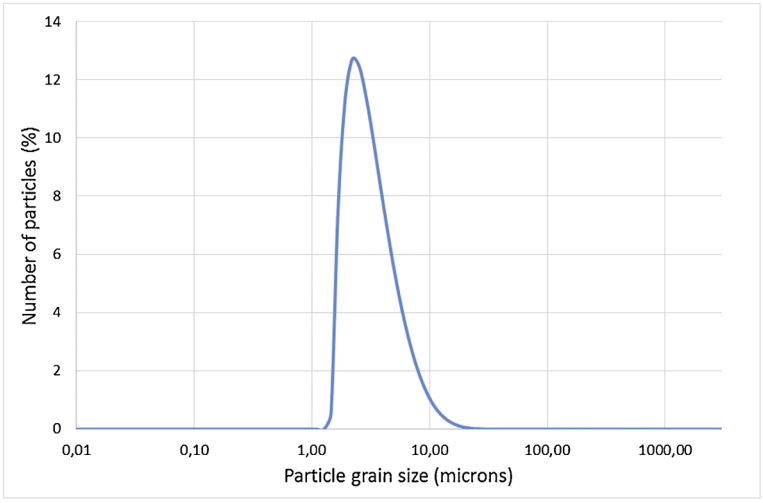

C

Fig. 1. SEM images: A) Ti_3SiC_2 powder, (magnification ×5000, scale bar 5 µm) B) Carbon fiber (magnification ×1000, scale bar 10 µm) C) Particle size distribution of the Ti_3SiC_2 powder.

Table 2
Summary of microstructure details and flexural strength of Ti_3SiC_2 composites spark plasma sintered at 1390 °C for 5 min.

REF	Type of fibers	vol% of fibers	Density (kg/m^3)	% of porosity	Flexural strength (MPa)
A	–	0	4.49	< 1	681 ± 8
B	HC-600	5	4.39	< 1	437 ± 7
C	HC-600	20	4.05	< 1	362 ± 10
D	HC-600	40	3.29	8	138 ± 10
E	XN-100	5	4.40	< 1	349 ± 6
F	XN-100	20	4.05	< 1	259 ± 5
G	XN-100	40	3.32	7	120 ± 8

matrix is very difficult and normally rows of fibers are present in the composite [26]. In this work, relatively short fibers (milled fibers) were used trying to achieve a homogeneous microstructure uniformly reinforced.

2. Methods

Ti_3SiC_2 powder (KANTHAL, purity 99%) was dry mixed with milled Pitch based carbon fibers (Nippon Graphite Fiber Corporation) to obtain composites with a fiber content of 5, 20 and 40 vol%. The mixing process was performed in a turbula-type mixer during 4 h and using alumina balls (ratio in weight 4:1) as milling media.

Two different types of fibers were used (see Table 1). A reference material without fiber was produced as well for comparison. The average size of both types of fibers was the same, 150 µm, the difference was in the thermal conductivity and electric resistivity. As in SPS the current path can be affected by the electrical and thermal conductivity of the material, the use of fibers with different electric and thermal conductivity can affect the local temperature obtained within the material and also the properties of the final product.

As shown in Fig. 1, Ti_3SiC_2 powder presents irregular shape and size lower than 30 µm with most of the particles are between 1 and 10 µm. The maximum length of the fibers declared by the supplier is 500 µm with a mean diameter of 11 µm.

The consolidation of the composites was performed by Spark Plasma

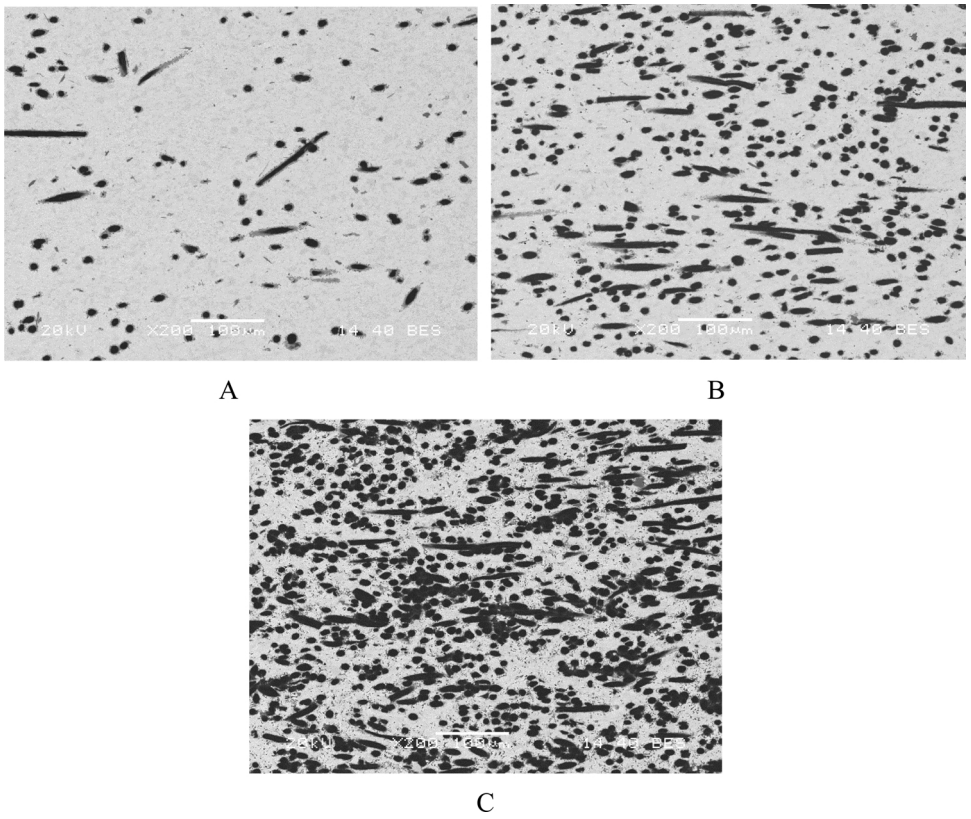

Fig. 2. SEM images of the Ti_3SiC_2 compositescontaining HC-600 Fibers (magnification ×200, scale bar 100 μm). A) Composite with 5 vol%, B 20 vol% and C) 40 vol % of carbon fibers.

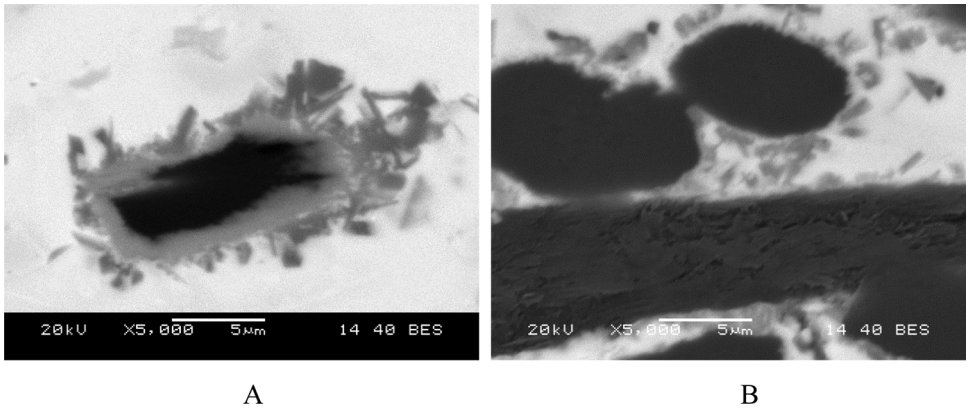

Fig. 3. SEM images of the Ti_3SiC_2 composites containing A) 5 vol% and B) 40 vol% of HC-600carbon fibers evidencing the different extent of fiber-matrix reaction zone (Magnification ×5000).

sintering (Model S8451, FCT). The powder was loaded into a 30 mm diameter graphite die in between two graphite punches. During the tests, the chamber was maintained under vacuum (10^{-2} Pa). Temperature was controlled by a pyrometer that measured the temperature in the interior of the graphite punch. For all composites, maximum temperature was 1390 °C with a holding time of 5 min. The load (50 MPa) was applied at room temperature and removed at the end of the dwell time. The temperature was selected based in preliminary tests trying to optimize the maximum possible density.

Density was measured by Archimedes' method using a Mettler AE 240 wt balance and porosity was analyzed according to the standard UNE-EN ISO 4605:1978. Microstructure and semi-quantitative chemical composition were analyzed by optical and SEM microscopy (Zeiss Nvision 40 and Zeiss EVO50). XRD analysis was carried out using a BRUKER D8 ADVANCE apparatus (Cu_Kα radiation, λ = 0.154 nm, 2θ = 20–100°, 40 kV – 30 mA, scan step 0.1°). 4-point bending tests were performed in an INSTRON machine according to the standard EN-843 – 1:2006. 3 bars with size 25 × 2.5 × 2 mm^3, length, by width by thickness, respectively, were tested for each composite. The thermal diffusivity was measured using a NETZSCH model 427 laser flash diffusivity apparatus in a dynamic argon atmosphere at a flow rate of 100 ml/min between 25 °C and 1500 °C. The specific heat measurements were conducted using a NETZSCH model DSC 404 F1 differential scanning calorimeter from 25 to 1500 °C in a high purity dynamic argon atmosphere. The thermal expansion was measured using a NETZSCH model 402 double pushrod dilatometer in He atmosphere at a flow rate of 50 ml/min. Particle size distribution was analyzed according to the standard ISO 13320-1 by laser diffraction in a Mastersizer 2000SM.

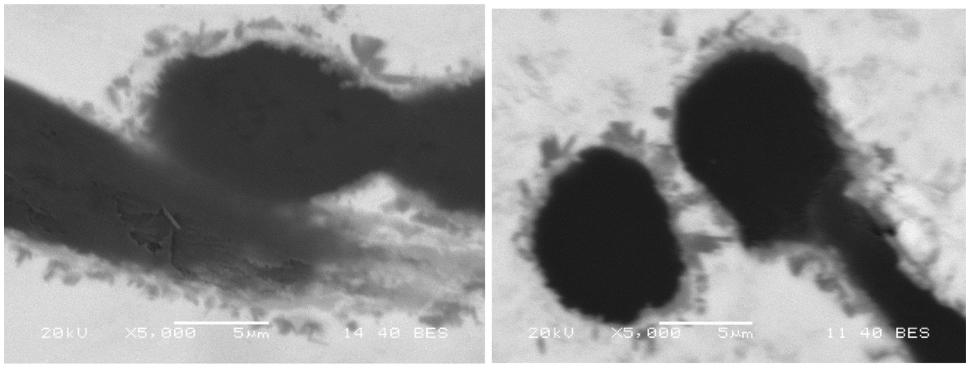

A B

Fig. 4. SEM images of the Ti_3SiC_2 composites with 20 vol% of carbon fibers showing similar reaction zone for both fiber type. A) HC-600 and B) XN-100 (Magnification ×5000).

3. Results and discussion

3.1. Microstructure

The density values obtained with the different composites are presented in Table 2. Density values close to the 99% of the theoretical value were achieved for composites containing up to 20 vol% of fibers, for the highest amount, 40 vol%, 7–8 vol% residual porosity remained trapped in the matrix.

The microstructure of composites with 5, 20 and 40 vol% of carbon fibers is shown in the polished cross sections of the obtained cylinders in Fig. 1. The Ti_3SiC_2 matrix is the light area and the carbon fibers the black circles and stripes. In the composites with 5 and 20 vol% of reinforcement, fibers are well distributed within the matrix. However, in the composite with 40 vol% of carbon fibers, some agglomerations can be observed. It is believed that the higher residual porosity of the composites with high content of fibers is linked to these agglomerations of fibers. No meaningful differences of fiber distribution were noticed using the HC-600 fiber type or XN-100 (Fig. 2).

A detailed microstructural analysis shows the interaction between the fibers and the matrix (see Fig. 3). The reaction between the fiber and the matrix depends on the amount of fibers in the composite. In the composites with 5 vol% of carbon fibers, about 1.5 ± 0.3 μm reaction zone is systematically observed at the fiber-matrix interface (grey area around the fiber, Fig. 3a, value presented is a mean of 100 measurements by SEM). However, in the composite with 40 vol% of carbon fibers this reaction zone is notably reduced, only small grey needles are observed, Fig. 3b.

The EDX analysis of the reaction zone confirms a Si rich phase with an important amount of carbon. When considering the Ti-Si-C phase diagram at the operating temperature [22] it is obvious that a reaction must occurs between Ti_3SiC_2 and carbon fibers as no tie-line exists between them. The reaction should lead to the formation of SiC and TiCx compounds.

The reason for this higher reactivity in the composites with lower amount of carbon fibers could depend on different factors. One of them is density. Densification is higher in the composites with low amount of carbon fibers and the porosity at the surface of the fiber could limit the reaction.

The same interaction was observed with both kind of fibers, as shown in Fig. 4. There is not a clear difference in microstructure using HC-600 or XN-100 fibers.

The decomposition of the Ti_3SiC_2 in a carbon rich environment was also confirmed by XRD. Fig. 5 shows the XRD pattern for a monolithic reference Ti_3SiC_2 material and a composite with 40 vol% of carbon fibers. Both materials were processed under the same SPS conditions. In both cases, main phases are Ti_3SiC_2 and TiC, but the amount of TiC is higher in the fiber containing composite, confirming enhanced decomposition of the matrix.

3.2. Mechanical properties

As expected from previous experience on materials containing various amount of short fiber [27,28] the introduction of fiber leads to strength decrease and this decrement is linear with increasing fiber volume content, owing to increased size and frequency of critical flaws seen by the material, i.e. the fiber themselves. The room temperature bending strength vary from about 680 MPa for monolithic Ti_3SiC_2 to around 120–140 MPa for the composites with the highest carbon fibers content (Table 2). With 20% of fibers, bending strength was around 400 MPa (Table 2), value in the range of conventional CMCs reinforced with chopped carbon fibers [29].

Similarly, the specific bending strength, defined as the ratio between strength and density, of the composites was affected by the volume of fibers (Fig. 6). The clear decrease of resistance observed in the composite with 40 vol% of fibers can be linked to the higher residual porosity of the material, about 10 vol% as compared to less than 1 vol% for composites with 5 and 20 vol% of fibers. The effect of the porosity seems to be more significant the higher reactivity observed in the composites with 5% of carbon fibers.

As for the effect of fiber type, any addition of XN100 leads to lower strength as compared to HC600. Since there are no remarkable differences in density or microstructure between the two series of composites and no data is available about the resistance of the fibers, it is difficult to ultimately propose an explanation for the observed behavior. In some cases, fibers with higher thermal conductivity (XN-100) present higher modulus but lower resistance.

Regarding the fracture mode of all composites is completely brittle and, rather than fiber pull-out, fiber tearing is mostly observed for both fiber type at any volume fraction. Fig. 7 shows indeed similar fracture surfaces of the composites with 5 and 40 vol% of HC carbon fibres.

The material with 40% of carbon fibers (HC-600) was selected for the characterization of the thermomechanical properties. Highly loaded CMCs are interesting for relatively high temperature applications (for ex, thermal protection systems up to a certain temperature). A certain degree of porosity (5–10) can play also a role increasing for example the thermal shock resistance [23].

The thermal expansion coefficient and the thermal conductivity of the material with 40 vol % of HC-600 carbon fibers were measured at different temperatures (see Table 3).

It is known form bibliography [30,31] that the CTE of Ti_3SiC_2 measured by dilatometry is around 9.1×10^{-6} C^{-1}. Values measured in this study present a clear reduction in CTE with values from 6.1 and 7.9×10^{-6} C^{-1} (RT to 1500 °C). Main reasons for that reduction are

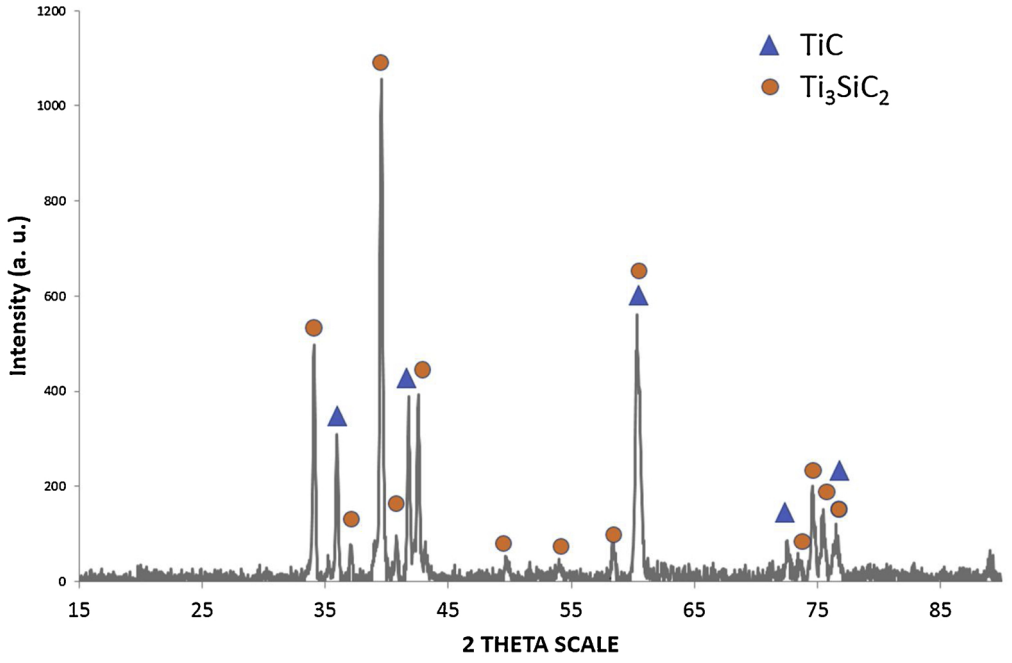

Fig. 5. XRD patterns of A) monolithic Ti_3SiC_2 and B) composite with 40 vol% of HC-600carbon fibers.

the presence of the fibers and some residual porosity in the composite.

The composite with the 40 vol% of carbon fibers show also a slight reduction in thermal conductivity compared to the pure MAX phase monolithic material: from 37 W/(m·K) of the monolithic material [30] to lower than 30 in the measured composite.

Fig. 8 shows the variation of the CTE with the temperature. An anomalous performance is observed at around 1200 °C with a decrease of the CTE increasing temperature. It is important to note that at temperatures higher than 1200 °C, the decomposition reaction of Ti_3SiC_2 is possible [22]. Then, the composition of the material changes as well as the tendencies in the values of CTE and thermal conductivity at higher temperatures.

4. Conclusions

This work presented the densification behavior and mechanical properties of Ti_3SiC_2- composites containing 0–40 vol% of short carbon fibers densified by Spark Plasma Sintering.

It was possible to obtain fully dense composites up to 20 vol% of carbon fibers and more than 90% of the theoretical density with the 40 vol % of fibers. To achieve densities higher than 90% in CMCs with this high amount of fibers is not trivial, as was stated in previous works [23].

There is a reaction between the fibers and the matrix, but the damage of the fibers is not very significant due to the short processing

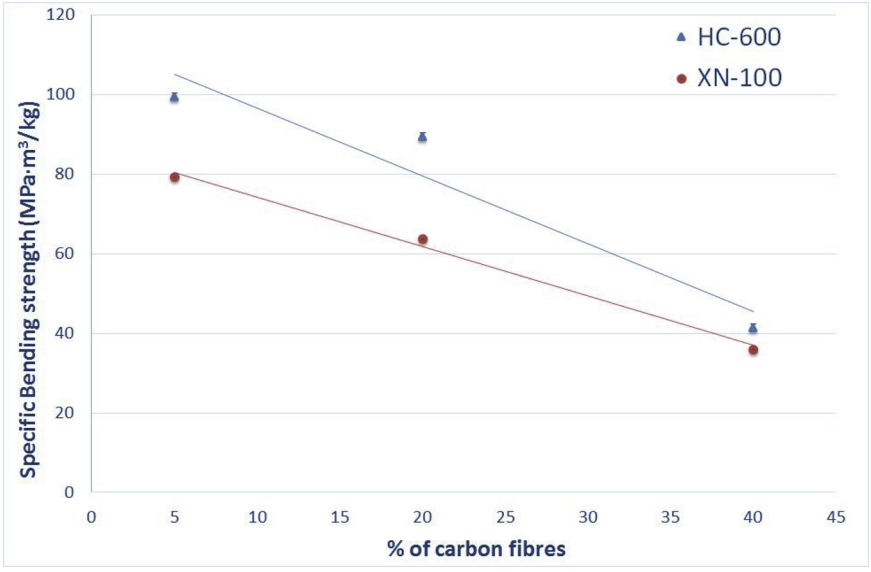

Fig. 6. Bending strength of the Ti_3SiC_2 composites with both kinds of fibers (HC-600 and XN-100).

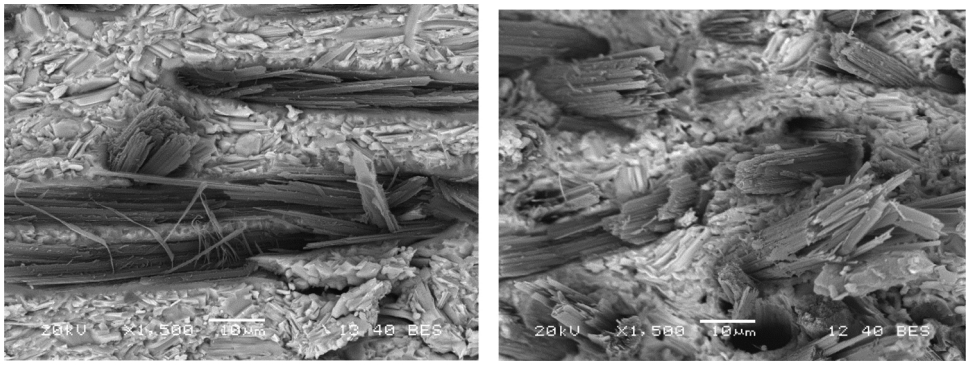

Fig. 7. SEM images of the fracture surfaces of composites containing A) 5 vol% and B) 40 vol% of HC-600 fibers.

Table 3
Thermo-mechanical properties of the composite with 40% of carbon fibers (HC-600).

Temperature (ºC)	CTE ($\cdot 10^{-6}$ /K^{-1})	Specific Heat (J/(g·K))	Thermal diffusivity (mm^2/s)	Thermal conductivity (W/(m·K))
50	6.1	0.73	11.5	29
500	7.4	1.12	6.3	24
1000	7.9	1.29	5.3	24
1500[a]	7.7[a]	1.65[a]	4.6[a]	26[a]

[a] Materials changes the composition at around 1200 °C.

time of SPS. The reaction zone extent depends on the matrix/fiber volume ratio, and in particular on the amount of released Si upon MAX decomposition during sintering.

Bending strength measured at room temperature linearly decreased as the fiber content increased.

With the addition of carbon fibers is possible to tailor the CTE and thermal conductivity of the Ti_3SiC_2 composites. The addition of fibers reduces the CTE and thermal conductivity at room temperature. In addition, the variation of the thermal properties up to 1500 °C was presented.

There are other properties like the thermal shock resistance that could be also positively affected by the addition of fibers [14].

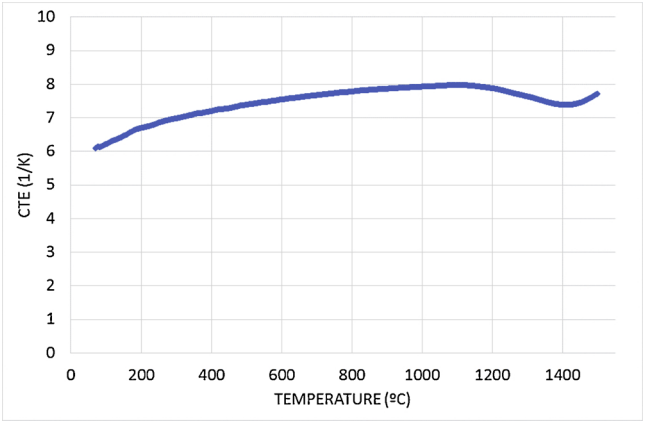

Fig. 8. Variation of the CTE with temperature (Ti3SiC2 + 40 Cf—HC600).

Acknowledgement

This work has received funding from the European Union's Horizon 2020 "Research and innovation programme" under grant agreement No 685594 (C^3HARME).

References

[1] M. Radovic, M.W. Barsoum, T. El-Raghy, J. Seidensticker, S. Wiederhorn, Tensile

properties of Ti3SiC2 in the 25-1300C temperature range, Acta Mater. 48 (2000) 453–459.
[2] Y.W. Bao, Y.C. Zhou, Mechanical properties of Ti3SiC2 at high temperature, Acta Metall. Sin. 17 (2004) 465–470.
[3] T. Zhen, M.W. Barsoum, S.R. Kalidindi, Effect of temperature, strain rate and grain size on the compressive properties of Ti3SiC2, Acta Mater. 53 (2005) 4163–4171.
[4] T. Zhen, M.W. Barsoum, S.R. Kalidindi, M. Radovic, Z.M. Sun, T. El-Raghy, Compressive creep of fine and coarse-grained Ti3SiC2 in air in the 1100–1300 °C temperature range, Acta Mater. 53 (2005) 4963–4973.
[5] H.B. Zhang, Y.W. Bao, Y.C. Zhou, Current status in layered ternary carbide Ti3SiC2, a review, J. Mater. Sci. Technol. 25 (1) (2009) 1–38.
[6] T.L. Ngai, L. Lu, J. Chen, J. Zhang, Y. Li, Preparation of SiC reinforced Ti3SiC2-base composite and its biocompatibility evaluation, Ceram. Int. 40 (2014) 5343–5348.
[7] L. Jaworska, M. Szutkowska, J. Morgiel, L. Stobierski, J. Lis, Ti3SiC2 as a bonding phase in diamond composites, J. Mater. Sci. Lett. 20 (2001) 1783–1786.
[8] E.N. Hoffman, D.W. Vinson, R.L. Sindelar, D.J. Tallman, G. Kohse, M.W. Barsoum, Max phase carbides and nitrides, properties for future nuclear power plant in-core applications and neutron transmutation analysis, Nucl. Eng. Des. 244 (2012) 11–24.
[9] L.H. Ho-Duc, T. El-Raghy, M.W. Barsoum, Synthesis and characterization of 0.3% fTiC–Ti3SiC2 and 0.3 vol% SiC–Ti3SiC2 composite, J. Alloys. Compd. 350 (1–2) (2003) 303–312 35J.
[10] F. Zhang, L.J. Wang, L. Shi, W. Jiang, L.D. Chen, Rapid fabrication of Ti3SiC2 nanocomposite using the spark plasma sintering-reactive (SPS-RS) method, Scr. Mater. 56 (3) (2007) 241–244.
[11] J.F. Zhang, T. Wu, L.J. Wang, W. Jiang, L.D. Chen, Microstructure and properties of Ti3SiC2/SiC nanocomposites fabricated by spark plasma sintering, Comp. Sci. Technol. 68 (2) (2008) 499–505.
[12] L. Silvestroni, D. Dalle Fabbriche, C. Melandri, D. Sciti, Relationships between Carbon fiber type and interfacial domain in ZrB2-based ceramics, J. Eur. Ceram. Soc. 36 (1) (2016) 17–24.
[13] J. Gonzalez-Juliana, J. Llorente, M. Bram, M. Belmonte, O. Guillon, Novel Cr2AlC MAX-phase/SiC fiber composites: synthesis, processing and tribological response, J. Eur. Ceram. Soc. 37 (2017) 467–475.
[14] L. Zoli, A. Vinci, P. Galizia, C. Melandri, D. Sciti, On the thermal shock resistance and mechanical properties of novel unidirectional UHTCMCs for extreme environments, Sci. Rep. 8 (1) (2018) 9148.
[15] A. Vinci, L. Zoli, D. Sciti, C. Melandri, S. Guicciardi, Understanding the mechanical properties of novel UHTCMCs through random forest and regression tree analysis, Mater. Des. 145 (2018) 97–107.
[16] P. Galizia, S. Failla, L. Zoli, D. Sciti, Tough salami-inspired Cf/ZrB2 UHTCMCs produced by electrophoretic deposition, J. Eur. Ceram. Soc. 38 (2) (2018) 403–409.
[17] F. Lenz, W. Krenkel, Fabrication of fiber composites with a MAX phase matrix by reactive melt infiltration, IOP Conf. Ser.: Mater. Sci. Eng 18 (2011) 202030.
[18] S. Chen, C. Zhang, Y. Zhang, H. Hu, Influence of pyrocarbon amount in C/C preform on the microstructure and properties of C/ZrC composites prepared via reactive melt infiltration, Mater. Des. 58 (2014) 570–576.
[19] X. Fan, X. Yin, L. Wang, L. Cheng, L. Zhang, Processing, microstructure and ablation behaviour of C/SiC–Ti3SiC2 composites fabricated by liquid silicon infiltration, Corros.Sci 74 (2013) 98–105.
[20] Q. Li, S. Dong, Z. Wang, G. Shi, Fabrication and properties of 3-D Cf/ZrB2-ZrC-SiC composites via polymer infiltration and pyrolysis, Ceram. Int. 39 (2013) 5937–5941.
[21] A. Paul, S. Venugopal, J.G.P. Binner, B. Vaidhyanathan, A.C.J. Heaton, P.M. Brown, UHTC–carbon fibre composites: preparation, oxyacetylene torch testing and characterization, J. Eur. Ceram. Soc. 33 (2013) 423–432, https://doi.org/10.1016/j.jeurceramsoc.2012.08.018.
[22] J. Zeng, S. Ren, J. Lu, Phase evolution of Ti3SiC2 annealing in vacuum at elevated temperatures, Int. J. Appl. Ceram. Technol. 10 (3) (2013) 527–539.
[23] L. Zoli, A. Vinci, L. Silvestroni, D. Sciti, M. Reece, S. Grasso, Rapid Spark Plasma Sintering to produce dense UHTCs reinforced with undamaged carbon fibres, Mater. Des. 130 (15) (2017) 1–7.
[24] M.A. El Saeed, F.A. Deorsola, R.M. Rashad, Influence of SPS parameters on the density and mechanical properties of sintered Ti3SiC2 powders, Int. J. Refract. Met. Hard Mater. 41 (2013) 48–53.
[25] B.Y. Liang, S.Z. Jin, M.Z. Wang, Low-temperature fabrication of high purity Ti3SiC2, J. Alloys. Compd. 460 (2008) 440–443.
[26] Z. Sun, H. Hashimoto, W. Tian, Y. Zou, Synthesis of the MAX phases by pulse discharge sintering, Int. J. Appl. Ceram. Technol. 7 (2010) 704–718.
[27] L. Pienti, D. Sciti, L. Silvestroni, S. Guicciardi, Effect of milling on the mechanical properties of chopped SiC fiber-reinforced ZrB2, Materials 6 (2013) 1980–1993.
[28] L. Silvestroni, D. Dalle Fabbriche, C. Melandri, D. Sciti, Relationships between Carbon fiber type and interfacial domain in ZrB2-based ceramics, J. Eur. Ceram. Soc. 36 (1) (2016) 17–24.
[29] B. Heidenreich, W. Krenkel (Ed.), “Melt Infiltration Process” Ceramic Matrix Composites, Willey VCH, Weinheim, Germany, 2008, pp. 113–139.
[30] M. Barsoum, et al., Thermal properties of Ti3SiC2, J. Phys. Chem. Solids 60 (4) (1999) 429–439.
[31] S.B. Li, J.X. Xie, L.T. Zhang, L.F. Cheng, Synthesis and some properties of Ti3SiC2 by hot pressing of Ti, Si and C powders part 2 – mechanical and other properties of Ti3SiC2, Mater. Sci. Technol. 21 (9) (2005) 1054–1058.